



HAL
open science

On the Characterization of Biofuels Cool Flame Products: Ethers

Philippe Dagaut, Nesrine Belhadj, Zahraa Dbouk, Roland Benoit

► **To cite this version:**

Philippe Dagaut, Nesrine Belhadj, Zahraa Dbouk, Roland Benoit. On the Characterization of Biofuels Cool Flame Products: Ethers. Twenty-first International Conference on Flow Dynamics, Institute of Fluid Science, Tohoku University, Nov 2024, Sendai, Japan. hal-04801450

HAL Id: hal-04801450

<https://hal.science/hal-04801450v1>

Submitted on 25 Nov 2024

HAL is a multi-disciplinary open access archive for the deposit and dissemination of scientific research documents, whether they are published or not. The documents may come from teaching and research institutions in France or abroad, or from public or private research centers.

L'archive ouverte pluridisciplinaire **HAL**, est destinée au dépôt et à la diffusion de documents scientifiques de niveau recherche, publiés ou non, émanant des établissements d'enseignement et de recherche français ou étrangers, des laboratoires publics ou privés.

Public Domain



Twenty-first International Conference on **Flow Dynamics**

November **18-20, 2024**
Sendai, Miyagi, Japan



Proceedings

On the Characterization of Biofuels Cool Flame Products: Ethers.

Philippe Dagaut¹, Nesrine Belhadj¹, Zahraa Dbouk¹, Roland Benoit¹.

¹CNRS, ICARE, 1-C avenue de la recherche scientifique, Orléans, 45071, France

ABSTRACT

Nowadays, ethers are considered as potential fuels or fuel additives. Here, the oxidation of a series of ethers was undertaken in a jet-stirred reactor at 10 bar in the cool-flame regime. The reacting mixtures were sampled and analyzed using high-resolution mass spectrometry (Orbitrap). Flow injection analyses were performed. Soft ionization (+/- heated electrospray and atmospheric pressure chemical ionization) were used. Numerous products were detected. Among them, chemical formulas corresponding to highly oxygenated molecules and oligomers were observed. A range of graphical tools was employed to characterize the oxidation products

1. Introduction

It is recognized that the combustion of fossil fuels contributes significantly to anthropogenically increasing emissions of CO₂ and particles in the atmosphere[1]. With the increasing global energy demand, socio-economic problems increase too[2]. Then, one needs to explore alternative energy sources among which renewable fuels from biomass are attractive [3-5]. Currently, ethers, which can be synthesized from bio-alcohols, are considered as potential fuels or fuel additives[6]. Whereas many studies concern the kinetics of oxidation of this class of fuels[4, 7, 8], the oxidation processes involved under cool-flame conditions are not well-characterized[9-19], in particular the formation of highly oxidized products deriving from complex processes which have been overlooked in combustion studies until advanced analytical techniques allowed their detection or characterization[19, 20].

The present work aims to better characterize the products of autoxidation of a series of ethers and extend the knowledge acquired in our previous works concerning the autoxidation of ethers [9, 10, 12-14, 21]. To this end, the oxidation of a series of ethers, namely diethyl ether (DEE), di-n-propyl ether (DPE), di-n-butyl ether (DBE), and tetrahydrofuran (THF), was undertaken in a jet-stirred reactor at 10 bar under cool-flame conditions. The reacting mixtures were sampled and analyzed using high-resolution mass spectrometry (Orbitrap). Analyses of the mass spectrometry data was performed using a range of graphical tools.

2. Method

The experiments were performed in a fused-silica JSR (Table 1) presented earlier [22, 23]. A 40 mm o.d. spherical sphere (35 cm³ internal volume) equipped with 4 injectors having nozzles of 1 mm i.d., for the admission of the gases achieving the stirring, constitutes the JSR. It is located inside a temperature-controlled oven of c.a. 1.5 kW, surrounded by insulating material. The JSR operates at 10 bar. N₂ and O₂ flow rates were measured and regulated by thermal mass-flow controllers. The liquid fuels were delivered by a HPLC pump and vaporized before injection into the reactor. A good thermal homogeneity along the whole vertical axis of the JSR was obtained in the experiments. The temperature was measured using a Pt/Pt-Rh10% thermocouple of 0.1 mm diameter located inside a thin-wall fused-silica tube (<0.5mm), which

prevents catalytic reactions on the metal wires.

Table 1 Experimental conditions.

Fuel	DEE	DPE	DBE	THF
Equivalence ratio	1	0.5	0.5–2	0.5
Pressure (bar)	10	10	10	10
Fuel mole fraction (ppm)	5000	1000	5000	5000
Residence time (s)	1	0.7	1	2
Temperature (K)	440–740	450–930	480–670	550–620
Bubbling time (min)	90	90	75	75

The high degree of dilution used in these experiments yielded a small temperature rise in the JSR. Samples of the reacting mixture were taken using a quartz probe connected to a cool acetonitrile tank (Fig. 1). The resulting solution was stored in a freezer at ~220 K for further analyses using soft ionization and high-resolution mass spectrometry (HRMS). Positive ($M + H^+ \rightarrow MH^+$) and negative ($MH \rightarrow M_{-H}^-$) were used for products identification.

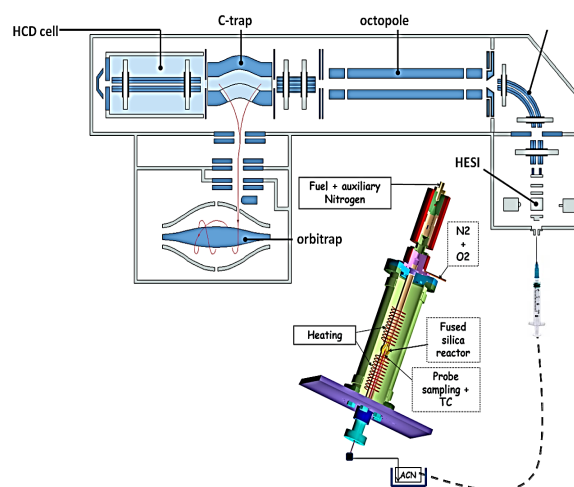


Fig. 1 Overview of the experimental setup used in the present study.

3. Results and Discussion

In Figures 2-4, one can see the variation of the mole fraction of the fuel as a function of temperature.

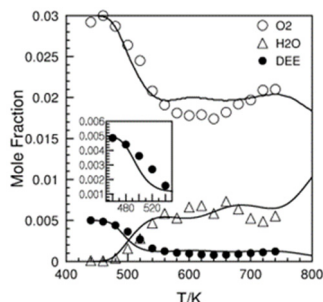


Fig. 2 Oxidation of 5000 ppm of DEE in a JSR at 10 bar.

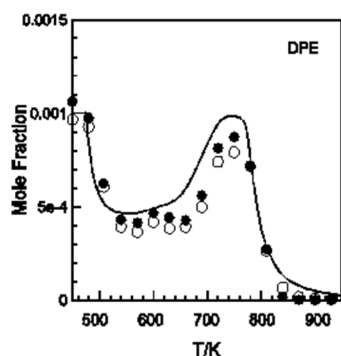


Fig. 3 DPE mole fraction profiles (symbols: data, lines: computations) as a function of reactor temperature in K at $\phi = 0.5, 0.7$ s, and 10 bar.

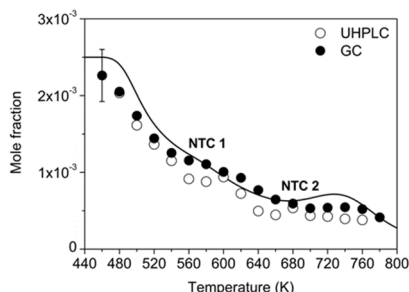


Fig. 4 DBE mole fraction profile during its oxidation at 10 atm (2500 ppm of DBE, $\phi = 2$ and residence time of 1s). The line corresponds to modeling results, symbols to GC and UHPLC experimental results (UHPLC-(+)APCI-HRMS, $C_8H_{19}O^+$, m/z 131.1430).

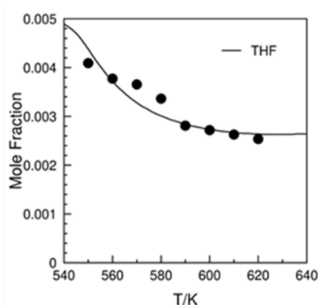
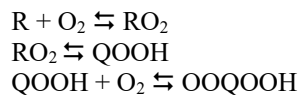
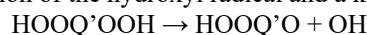


Fig. 5 Consumption of THF based on m/z 73.0647 ($C_4H_9O^+$). The data (dots) are compared to simulations (lines).

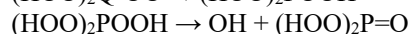
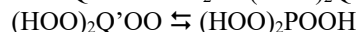
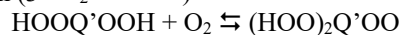
One can observe that all the fuels considered here show a cool-flame oxidation regime. The formation of ketohydroperoxides and highly oxygenated compounds resulting from third O_2 addition on the fuels radicals (R) was observed. Their formation occurs via a sequence of reactions described below:



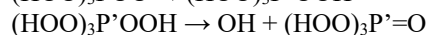
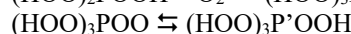
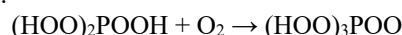
$OOQOOH \rightleftharpoons HOOQ'OOH$ followed by the formation of the hydroxyl radical and a ketohydroperoxide:



Dihydroperoxides can also react with molecular oxygen (3^{rd} O_2 addition):



The reaction can also proceed through a 4^{th} O_2 addition:



In Figures 6-9, one can observe the formation of ketohydroperoxides from the oxidation of the fuels considered in this work.

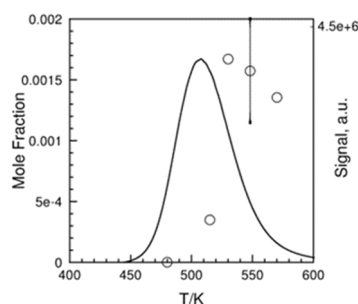


Fig. 6 Formation of $C_4H_9O_4^+$ (m/z 121.0492) ion during the oxidation of DEE in a JSR. Analyses were performed in FIA and APCI (+)

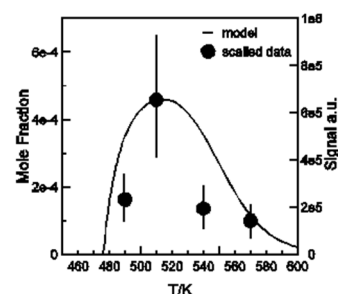


Fig. 7 Comparison between experimental (symbols) and computed total mole fraction of KHPs (1000 ppm of DPE, $\phi = 0.5, 0.7$ s, and 10 atm). The data are scaled to the computed maximum concentration.

As can be seen from these figures, KHPs reach a maximum mole fraction at temperatures ranging from 510 to 560 K.

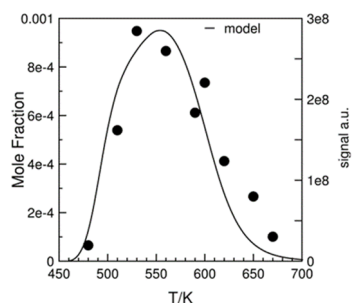


Fig. 8 Formation of KHPs from DBE oxidation. The data were obtained by integration of UHPLC-MS signal and scaled to the computed maximum experimental concentration.

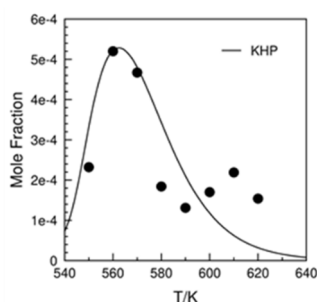


Fig. 9 Formation of $C_4H_6O_4$ in a JSR by oxidation of 5000 ppm of THF. Analyses were performed in FIA and APCI (+) mode. The data (dots) represent the signal recorded at m/z 119.0338 ($C_4H_7O_4^+$), scaled to the KHPs maximum computed mole fraction.

As indicated earlier, many oxygenated products were observed under cool flame conditions. In order to represent this large dataset, Van Krevelen plots using our HRMS data were used to compare products formation during the oxidation of the four ethers. An example of such results is given in Figure 10 where the double bond equivalent number was computed ($1 + C - H/2 - O$, where C , H , and O stand for the number of carbon, hydrogen, and oxygen atoms, respectively).

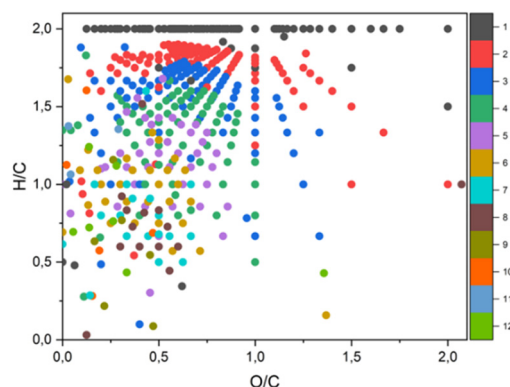


Fig. 10 Van Krevelen plot for DBE oxidation products using HRMS data (sample taken at 530 K). The color coding indicates the double bond equivalent number in the detected chemical formulas.

Chemical formulas with $H/C > 0.7$ and $O/C < 0.25$

should correspond to aromatics.

4. Concluding Remarks

A large set of complex products of oxidation of four ethers (DEE, DPE, DBE, and THF) was detected in a JSR under cool-flame conditions using high-resolution mass spectrometry. They range from ketohydroperoxides to highly oxygenated products. Van Krevelen plots indicated the likely presence of aromatics in the products.

Acknowledgements

Research funded by the Labex Caprysses (ANR-11-LABX-0006-01).

References

- [1] J. Lelieveld; K. Klingmüller; A. Pozzer; R. T. Burnett; A. Haines; V. Ramanathan, *P.N.A.S.* 116 (2019) 7192-7197.
- [2] C. Olson; F. Lenzmann, *MRS Energy & Sustainability* 3 (2016) 6.
- [3] A. Muscat; E. M. de Olde; I. J. M. de Boer; R. Ripoll-Bosch, *Global Food Security* 25 (2020) 100330.
- [4] B. Rotavera; C. A. Taatjes, *Prog. Energy Combust. Sci.* 86 (2021) 100925.
- [5] L. Cai; F. vom Lehn; H. Pitsch, *Energy Fuels* 35 (2021) 1890-1917.
- [6] M. Martinez; X. Duret; D. Pham Minh; A. Nzihou; J.-M. Lavoie, *Int.l J. Energy Prod. Manage.* 4 (2019) 298-310.
- [7] L. S. Tran; O. Herbinet; H. H. Carstensen; F. Battin-Leclerc, *Prog. Energy Combust. Sci.* 92 (2022) 1019-1019.
- [8] M. N. Romanias; M. M. Coggon; F. Al Ali; J. B. Burkholder; P. Dagaut; Z. Decker; C. Warneke; C. E. Stockwell; J. M. Roberts; A. Tomas; N. Houzel; C. Coeur; S. S. Brown, *ACS Earth Space Chem.* 8 (2024) 857-899.
- [9] N. Belhadj; R. Benoit; P. Dagaut; M. Lailliau; Z. Serinyel; G. Dayma; F. Khaled; B. Moreau; F. Foucher, *Combust. Flame* 222 (2020) 133-144.
- [10] Z. Serinyel; M. Lailliau; G. Dayma; P. Dagaut, *Fuel* 263 (2020) 16554-16554.
- [11] Z. D. Wang; N. Hansen; A. W. Jasper; B. J. Chen; D. M. Popolan-Vaida; K. K. Yalamanchi; A. Najjar; P. Dagaut; S. M. Sarathy, *Combust. Flame* 219 (2020) 384-392.
- [12] N. Belhadj; R. Benoit; P. Dagaut; M. Lailliau; Z. Serinyel; G. Dayma, *Proc. Combust. Inst.* 38 (2021) 337-344.
- [13] N. Belhadj; R. Benoit; M. Lailliau; V. Glasziou; P. Dagaut, *Combust. Flame* 228 (2021) 340-350.
- [14] N. Belhadj; M. Lailliau; R. Benoit; P. Dagaut, *Molecules* 26 (2021) 7174.
- [15] D. M. Popolan-Vaida; A. J. Eskola; B. Rotavera; J. F. Lockyear; Z. D. Wang; S. M. Sarathy; R. L. Caravan; J. Zador; L. Sheps; A. Lucassen; K. Moshhammer; P. Dagaut; D. L. Osborn; N. Hansen; S. R. Leone; C. A. Taatjes, *Angew. Chem.-Int. Ed.* 61 (2022) 9168-9168.
- [16] C. Xie; M. Lailliau; G. Issayev; Q. Xu; W. Chen; P. Dagaut; A. Farooq; S. M. Sarathy; L. Wei; Z. Wang,

- Combust. Flame* 242 (2022) 112177.
- [17] Z. Dbouk; N. Belhadj; M. Lailliau; R. Benoit; G. Dayma; P. Dagaut, *Fuel* 350 (2023) 28865.
- [18] B. Z. Liu; Q. M. Di; M. Lailliau; N. Belhadj; P. Dagaut; Z. D. Wang, *Combust. Flame* 254 (2023) 12813-12813.
- [19] Z. Dbouk; N. Belhadj; M. Lailliau; R. Benoit; P. Dagaut, *Fuel* 358 (2024) 130306.
- [20] Z. Wang; D. M. Popolan-Vaida; B. Chen; K. Moshhammer; S. Y. Mohamed; H. Wang; S. Sioud; M. A. Raji; K. Kohse-Höinghaus; N. Hansen; P. Dagaut; S. R. Leone; S. M. Sarathy, *P.N.A.S.* 114 (2017) 13102-13107.
- [21] N. Belhadj; R. Benoit; P. Dagaut; M. Lailliau, *Energy Fuels* 35 (2021) 7242–7252.
- [22] T. Le Cong; P. Dagaut; G. Dayma, *J. Eng. Gas Turbines and Power* 130 (2008) 041502-10.
- [23] P. Dagaut; M. Cathonnet; J. P. Rouan; R. Foulatier; A. Quilgars; J. C. Boettner; F. Gaillard; H. James, *J. Phys. E-Sci. Instrum.* 19 (1986) 207-209.